

Ba₂Y(Nb/Ta)O₆-Doped YBCO Films on Biaxially Textured Ni-5at.% W Substrates

Max Sieger, Patrick Pahlke, Jens Hänisch, Maria Sparing, Marco Bianchetti, Judith MacManus-Driscoll, Mayraluna Lao, Michael Eisterer, Alexander Meledin, Gustaaf Van Tendeloo, Rainer Nast, Ludwig Schultz, Bernhard Holzapfel, and Ruben Hühne

Abstract—The incorporation of nanoscaled pinning centers in superconducting YBa₂Cu₃O_{7-δ} (YBCO) films is one of the core topics to enhance the critical current density $J_c(B, \Theta)$ of coated conductors. The mixed double-perovskite Ba₂Y(Nb/Ta)O₆ (BYNTO) can be grown in nanosized columns parallel to the YBCO c -axis and in steplike patterns, making it customizable to meet specific working conditions (T, B, Θ). We compare a 1.6 μm thick film of pure YBCO and a similar film with additional 5 mol% of BYNTO, grown by pulsed laser deposition with a growth rate of 1.6 nm/s on chemically buffered biaxially textured Ni-5at.% W tape. Our doped sample shows nanosized BYNTO columns parallel to c_{YBCO} and plates in the ab -plane containing Y, Nb, and Ta. An improved homogeneity of the critical current density J_c over the sample was evaluated from trapped field profiles measured with a scanning Hall probe microscope. The mean J_c in the rolling direction of the tape is 1.8 MA/cm² (77 K, self-field) and doubles the value of the undoped sample. Angular-dependent measurements of the critical current density, $J_c(\Theta)$, show a decreased anisotropy of the doped film for various magnetic fields at 77 K and 64 K.

Index Terms—BYNTO, pinning, pulsed laser deposition, RABiTS, YBCO.

I. INTRODUCTION

THE use of high-temperature superconductors such as YBa₂Cu₃O_{7-δ} (YBCO) in applications as fault current limiters, motors, generators and high-field magnets, e.g. for

fusion reactors, is limited by the current carrying capability in external magnetic fields. The immobilization of vortices at natural or artificial pinning centers (APCs) in the superconductor leads to an enhancement of the critical current I_c [1], [2]. APCs can be created in several ways, e.g. incorporation of nanoparticles/nanocolumns by pulsed laser deposition (PLD) via multilayer deposition [3]–[5] or mixed targets [6]–[10], in chemical solution deposition via addition of the respective salts in the solution [11] or other methods [12], [13]. Size, shape, density and distribution of the APCs are key parameters for tailoring the critical current density $J_c(T, B, \Theta)$ and can be adjusted to reach the favored performance in certain magnetic field and temperature regimes. A lower anisotropy is desirable for high-field coils based on superconducting tapes, where the lowest value of $I_c(B, \Theta)$ is the limiting criterion for applications.

The mixed double-perovskite Ba₂Y(Nb/Ta)O₆ (BYNTO) is a strong candidate for high pinning forces as it can be grown in different manners: straight BYNTO nanocolumns lead to very high J_c values in magnetic fields up to 9 T, pinning forces among the highest values reported, and strong matching effects in $J_c(B, \Theta)$ [9]. Step-like patterns of BYNTO inside the YBCO matrix give additional peaks in $J_c(B, \Theta)$ and perform better than similar pure or single-doped YBCO samples [10].

Our goal is to transfer these structures onto technical rolling-assisted biaxially textured substrates (RABiTS), which are produced in an industrial scale. Here, we present the structural and electrical properties of a 5 mol% BYNTO doped YBCO (BYNTO:YBCO) film, deposited on biaxially textured Ni-5at.% W (Ni5W) [14] tape by means of X-Ray diffraction, scanning and transmission electron microscopy, scanning Hall probe microscopy and transport current measurements.

II. EXPERIMENTAL DETAILS

A. Sample Preparation

YBCO films with a thickness of 1.6 μm were grown on biaxially textured Ni5W tapes of 80 μm thickness with a chemically deposited buffer layer system of ~270 nm thick La₂Zr₂O₇ and ~30 nm thin CeO₂ by PLD using a Lambda Physics LPX305Pro KrF excimer laser ($\lambda = 248$ nm) with an energy density of 1.6 J/cm² at the target surface. At a pulse frequency of 10 Hz we achieve a mean growth rate of 1.6 nm/s. All targets were prepared from precursor powder mixtures according to the stoichiometry of undoped YBCO and YBCO with additional

2.5 mol% Ba_2YNbO_6 and 2.5 mol% Ba_2YTaO_6 by pressing and sintering at 950 °C in flowing oxygen for 24 h. Deposition took place in an atmosphere of 0.4 mbar of flowing oxygen at 830 °C substrate temperature, which yielded highest values of inductive critical temperature, T_c , and J_c in preliminary tests. Oxygen loading of the films was carried out at 765 °C for 1 h in 400 mbar O_2 before cooling to room temperature. A silver cap layer of several 10 nm thickness was deposited on top to lower the contact resistance and protect the films.

B. Structural Characterization

Transmission electron microscopy (TEM) was carried out on an FEI Osiris microscope operated at 200 kV as well as on an FEI Titan³ electron microscope operated at 200 kV and 300 kV for high angle annular dark field scanning transmission electron microscopy (HAADF-STEM) and energy dispersive X-ray spectroscopy (EDX).

The crystal structure was analyzed with a Bruker D8 Advance diffractometer (Co anode) in modified parallel-beam geometry (Θ -2 Θ scans). The c -axis parameter of YBCO was calculated from the peak positions of the (00ℓ) peaks by the Nelson-Riley formalism [15]. Pole figures of the YBCO (103) ($2\Theta = 32.5^\circ$) and BYNTO (220) ($2\Theta = 29.9^\circ$) [16] planes were taken at a Philip X'Pert PW3040 (Cu anode).

C. Electrical Properties

The critical temperature $T_{c,50}$ and the transition width $\Delta T_c (= T_{c,90} - T_{c,10})$ were measured inductively. Trapped field profile measurements were carried out to determine the local critical current, for detailed procedure see Ref. [17].

Angle-resolved transport current measurements in magnetic fields, $J_c(B, \Theta)$ with $\Theta = 0\text{--}240^\circ$ being the angle between magnetic field \mathbf{B} and sample normal \mathbf{n} ($\mathbf{B} \parallel \mathbf{n}$ for 0° and 180° , $\mathbf{B} \perp \mathbf{n}$ for 90°), were conducted in maximum Lorentz force configuration in a four-point measurement assembly on laser-cut bridges [18] of 800 μm length and 300 μm width. Here, J_c is defined by an electrical field criterion of 1 $\mu\text{V}/\text{cm}$.

III. RESULTS AND DISCUSSION

A. Structural Properties

The orientation of the grown films was studied with X-ray diffraction. The appearance of only high-intensity (00ℓ) peaks of YBCO in the Θ -2 Θ scans proves the growth of highly c -axis oriented films on the chemically buffered Ni5W tapes, Fig. 1. An additional peak of the dopant is observed for BYNTO:YBCO, which is significantly broader and asymmetric. This might arise from the overlapping of different peaks of particle species with varying stoichiometry. Similar effects for Y-rich nanoparticles were reported by Reich *et al.* [5]. This is also supported by the variation in the nanoparticle stoichiometry shown in the TEM-EDX data, Fig. 2. Two types of phases related to the dopant form inside the YBCO matrix. A few BYNTO columns (cf. Fig. 2, Nb and Ta enriched areas

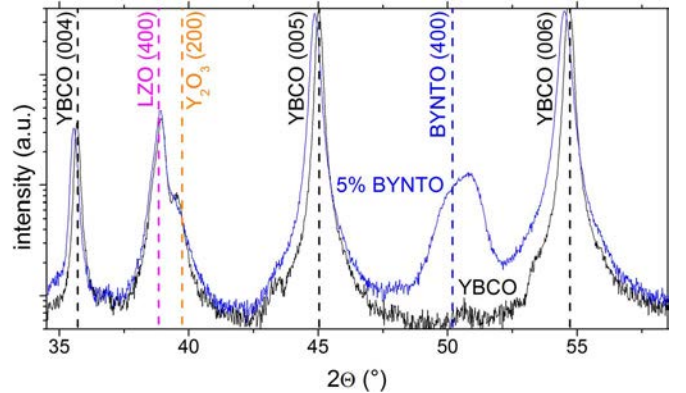


Fig. 1. X-ray diffraction pattern (Co- K_α) of pure YBCO and 5 mol% BYNTO:YBCO on Ni5W: dashed lines indicate theoretical peak positions.

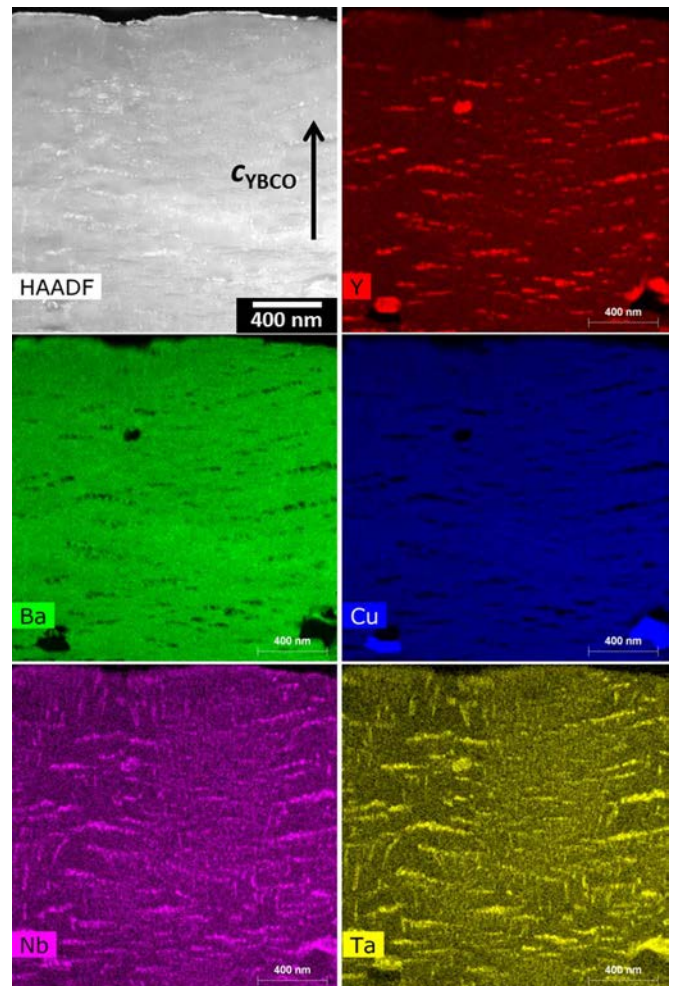


Fig. 2. HAADF-STEM image and respective TEM-EDX mappings for Y (red), Ba (green), Co (blue), Nb (purple), and Ta (yellow) for 5 mol% BYNTO:YBCO on Ni5W tape.

with a Y content similar to the surrounding YBCO matrix) with a diameter of ~ 10 nm grow with a certain splay around the YBCO c -axis direction. Furthermore, we find large plates parallel to the YBCO ab -plane, which are rich in Y and Cu-depleted. These might be Nb and Ta enriched Y_2O_3 plates, stacks of Y_2O_3 /BYNTO or the respective single-perovskites.

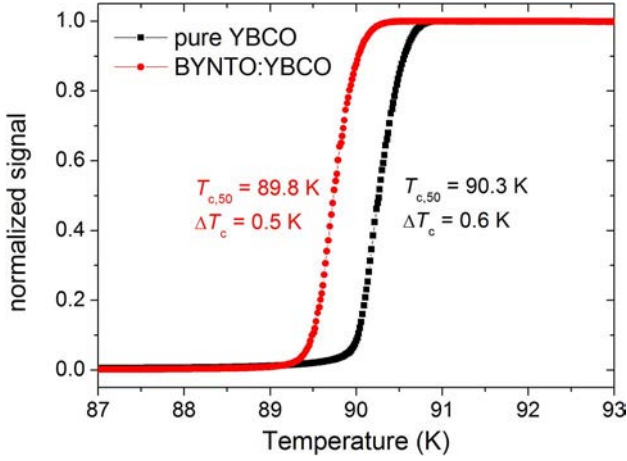


Fig. 3. Superconducting transition of pure YBCO and 5 mol% BYNTO:YBCO on Ni5W tape.

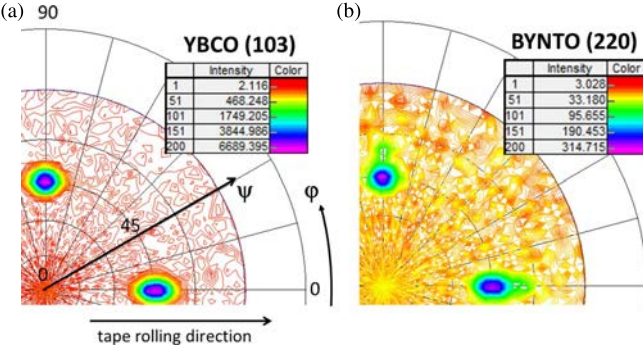


Fig. 4. Pole figures of the (a) YBCO (103) and (b) BYNTO (220) plane for 5 mol% BYNTO:YBCO on Ni5W tape.

This microstructure with few nanocolumns and large plates is different from the results of BYNTO-doped YBCO on SrTiO₃ (STO) substrates [9], [10]. The discrepancy is very likely a result of the chosen deposition parameters (high substrate temperature, high growth rate). Modified deposition temperatures and/or growth rates can produce more columnar or meandering structures.

A detailed analysis of the diffraction patterns indicates a change of the YBCO *c*-axis length from 11.69 Å (undoped) to 11.72 Å (doped). As T_c remains almost uninfluenced by BYNTO-doping (Fig. 3), a reduced oxygen content in the YBCO matrix is unlikely to account for the peak shift of the YBCO peaks to lower 2θ values for the doped sample. The larger *c*-axis might be explained by a stretching of the YBCO lattice in *c*-direction in order to match three unit cells of the cubic dopant ($a_{\text{BYNTO}} = 8.33$ Å) to two unit cells of YBCO ($c_{\text{YBCO}} = 11.68$ Å) by incorporating misfit dislocations similar to BHO-doped YBCO [19]. However, this needs to be confirmed with high-resolution TEM.

Texture measurements were performed to study the in-plane alignment of the films. High intensities at $\varphi = 0^\circ$ and 90° along $\psi = 45^\circ$ in the YBCO (103) and BYNTO (220) pole figures (Fig. 4) indicate a biaxially oriented growth of the dopant inside the YBCO matrix. The poles are elongated along the rolling direction of the tape. Similar results were observed previously for thin YBCO films on such tapes [20]. The texture quality,

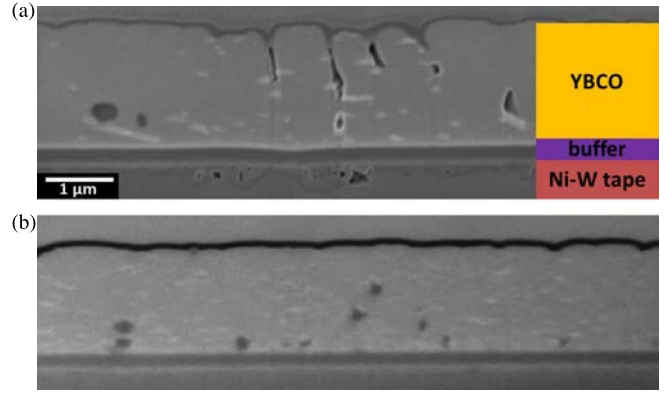


Fig. 5. Secondary electron images of cross sections of (a) pure YBCO and (b) 5 mol% BYNTO:YBCO on Ni5W tape. The enhancement of surface flatness and refinement of nanoparticles by BYNTO addition are apparent.

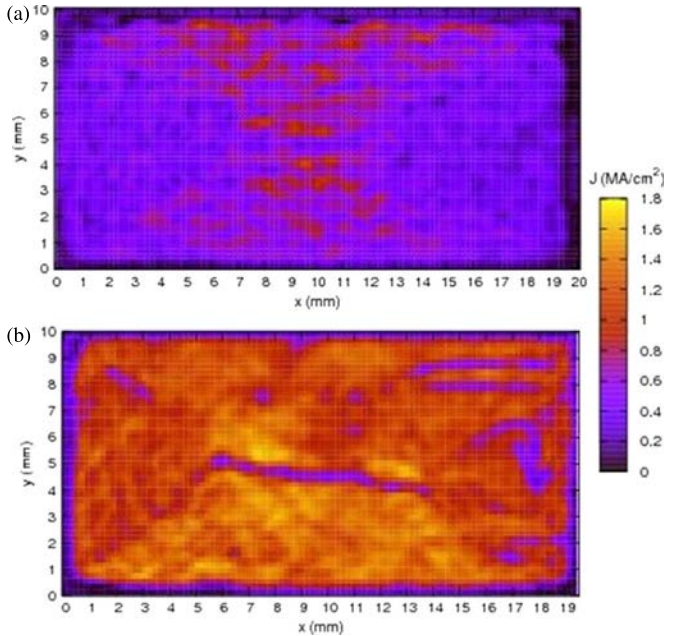


Fig. 6. Critical current density maps evaluated from trapped field profiles at 77 K for (a) pure YBCO and (b) 5 mol% BYNTO:YBCO on Ni5W tape.

i.e., peak width in φ and ψ direction, of all samples is in the typical range for YBCO on NiW tapes and not influenced by the dopant.

The secondary electron images of cross-sectional cuts on pure and BYNTO-doped YBCO (Fig. 5) show the surface flattening effect of the BYNTO addition to the YBCO matrix. No deep trenches are observed in the doped film (Fig. 5(b)) which also shows less porosity and a refinement of large Y_2O_3 precipitates (bright spots in the YBCO layer, Fig. 5(a)).

B. Electrical Properties

The BYNTO:YBCO sample has a T_c very close to the value of undoped YBCO with a sharp transition width (<1K) (Fig. 3). The critical current density maps, obtained from remanent field profiles on the complete sample surface, Fig. 6, show a doubling of the average self-field J_c in rolling direction of the tape at 77 K for the doped sample (1.8 MA/cm^2)

TABLE I
AVERAGE $J_{c,x}$ (ROLLING DIRECTION) AND $J_{c,y}$ (TRANSVERSE DIRECTION) OF PURE YBCO AND 5 MOL% BYNTO:YBCO ON Ni5W TAPE

BYNTO CONTENT (MOL%)	$J_{c,x}$ (MA/cm ²)	$J_{c,y}$ (MA/cm ²)	$J_{c,y}/J_{c,x}$
0	0.9±0.2	0.5±0.1	0.6
5	1.8±0.2	1.5±0.2	0.8

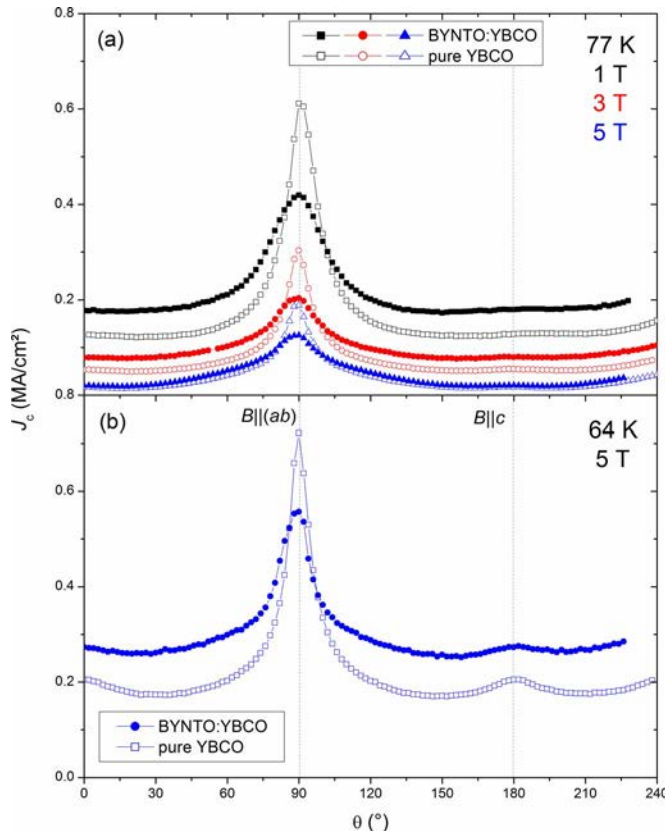


Fig. 7. Anisotropy of pure YBCO and 5 mol% BYNTO:YBCO on Ni5W tape at (a) 77 K and (b) 64 K, for different magnetic fields.

compared to the pure YBCO (0.9 MA/cm²) with a significantly reduced difference of $J_{c,x}$ to $J_{c,y}$ (Fig. 6 and Table I). The reason for this improvement might be the lower surface roughness, avoiding deep trenches and increasing the effective cross-section of the superconducting film, and the optimized microstructure with less pores and refined precipitates (cf. Fig. 5). Additionally, BYNTO might also enhance the pinning inside the grain boundaries as shown by Tsuruta *et al.* for BHO-doped superconducting films [21], yet this point needs further analysis. The difference of J_c along the x and y direction has two reasons. First, the grains in RABiTS tapes such as Ni5W are usually slightly elongated in rolling direction, leading to a better current percolation in this direction due to larger grain boundary areas (“brick wall model”) and a larger number of grains per width (percolation threshold) [22]. Second, possible macroscopic defects such as grooves or scratches related to the rolling process of the tape may hinder current flow in transverse direction.

BYNTO doping enhances the critical current density $J_c(\Theta)$ over a wide angular range of the applied magnetic field (Fig. 7).

TABLE II
 $J_c^{\text{Max}}/J_c^{\text{Min}}$ OF PURE YBCO AND 5 MOL% BYNTO:YBCO ON Ni5W TAPE FOR SEVERAL TEMPERATURES AND MAGNETIC FIELDS

BYNTO CONTENT (MOL%)	ANISOTROPY ($J_c^{\text{MAX}}/J_c^{\text{MIN}}$)			
	77 K 1 T	77 K 3 T	77 K 5 T	64 K 5 T
0	5.1	6.1	13.9	4.2
5	2.5	2.7	6.9	2.2

Whereas J_c for magnetic fields parallel to the tape surface ($\pm 10^\circ$ around $B \parallel ab$) is slightly decreased, J_c is enhanced for all other directions. Most probably the randomly distributed Y_2O_3 nanoparticles are responsible for this matter. A pronounced c -axis peak ($B \parallel c_{\text{YBCO}}$) is not visible at 77 K (Fig. 7(a)) but is clearly observed at lower temperatures (65 K, Fig. 7(b)) for both, the doped and the undoped film. The small amount of c -axis-oriented nanocolumns is most likely causing the peak for the BYNTO-doped sample, in the case of pure YBCO it might be due to correlated dislocations. The decrease and broadening of the J_c peak for $B \parallel ab$ of the BYNTO-doped sample is related to the splay of the $\text{Y}_2\text{O}_3/\text{BYNTO}$ platelets around the ab -direction (Fig. 2), resulting in a wider angular range for vortices to lock in.

However, BYNTO:YBCO shows a reduced anisotropy at different temperature and magnetic field regimes (Table II), e.g. the minimum J_c is 50% higher for the doped film at 77 K, 1 T.

CONCLUSION

In this paper, we demonstrated the capability of producing 1.6 μm thick 5 mol% BYNTO:YBCO films on fully CSD-buffered Ni5W substrates with a reasonable growth rate. Nano-sized BYNTO columns parallel to the YBCO c -axis and Nb and Ta enriched Y_2O_3 plates or stacks of $\text{Y}_2\text{O}_3/\text{BYNTO}$ parallel to the YBCO ab -plane are incorporated with biaxial orientation into the YBCO matrix. Inductive measurements show a critical temperature of 90 K and a very uniform average critical current density of 1.8 MA/cm² along the tapes rolling direction. BYNTO doping enhances the critical current in a wide range of magnetic field orientations. At lower temperatures (65 K), a c -axis peak becomes visible. Adjustment of the deposition parameters temperature and growth rate might further enhance the $J_c(B, \Theta)$ characteristics of BYNTO-doped YBCO films on biaxially textured Ni-W tapes.

ACKNOWLEDGMENT

The authors would like to thank M. Falter of Deutsche Nanoschicht GmbH for providing the buffered Ni5W template and M. Kühnel, U. Fiedler, and J. Scheiter for technical assistance.

REFERENCES

- [1] T. Matsushita, “Flux pinning in superconducting 123 materials,” *Supercond. Sci. Technol.*, vol. 13, no. 6, pp. 730–737, Feb. 2000.
- [2] K. Matsumoto and P. Mele, “Artificial pinning center technology to enhance vortex pinning in YBCO coated conductors,” *Supercond. Sci. Technol.*, vol. 23, no. 1, Dec. 2009, Art. no. 014001.

- [3] T. Haugen, P. N. Barnes, R. Wheeler, F. Meisenkothen, and M. Sumption, “Addition of nanoparticle dispersions to enhance flux pinning of the $\text{YBa}_2\text{Cu}_3\text{O}_{7-x}$ superconductor,” *Nature*, vol. 430, no. 7002, pp. 867–870, Aug. 2004.
- [4] A. Kiessling *et al.*, “Nanocolumns in $\text{YBa}_2\text{Cu}_3\text{O}_{7-x}/\text{BaZrO}_3$ quasi-multilayers: Formation and influence on superconducting properties,” *Supercond. Sci. Technol.*, vol. 24, no. 5, Mar. 2011, Art. no. 055018.
- [5] E. Reich *et al.*, “Structural and pinning properties of $\text{Y}_2\text{Ba}_4\text{CuMO}_y$ ($M = \text{Nb}, \text{Zr}$)/ $\text{YBa}_2\text{Cu}_3\text{O}_{7-\delta}$ quasi-multilayers fabricated by off-axis pulsed laser deposition,” *Supercond. Sci. Technol.*, vol. 22, no. 10, Aug. 2009, Art. no. 105004.
- [6] C. Cai, B. Holzapfel, J. Hänisch, L. Fernández, and L. Schultz, “Magnetotransport and flux pinning characteristics in $\text{RBa}_2\text{Cu}_3\text{O}_{7-\delta}$ ($R = \text{Gd}, \text{Eu}, \text{Nd}$) and $(\text{Gd}_{1/3}\text{Eu}_{1/3}\text{Nd}_{1/3})\text{Ba}_2\text{Cu}_3\text{O}_{7-\delta}$ high- T_c superconducting thin films on SrTiO_3 ,” *Phys. Rev. B, Condens. Matter Mater. Phys.*, vol. 69, no. 10, Mar. 2004, Art. no. 104531.
- [7] J. L. MacManus-Driscoll *et al.*, “Strongly enhanced current densities in superconducting coated conductors of $\text{YBa}_2\text{Cu}_3\text{O}_{7-x} + \text{BaZrO}_3$,” *Nat. Mater.*, vol. 3, no. 7, pp. 439–443, Jul. 2004.
- [8] D. M. Feldmann *et al.*, “Improved flux pinning in $\text{YBa}_2\text{Cu}_3\text{O}_7$ with nanorods of the double perovskite Ba_2YNbO_6 ,” *Supercond. Sci. Technol.*, vol. 23, no. 9, Jul. 2010, Art. no. 095004.
- [9] L. Ophérdén *et al.*, “Large pinning forces and matching effects in $\text{YBa}_2\text{Cu}_3\text{O}_{7-\delta}$ thin films with $\text{Ba}_2\text{Y}(\text{Nb/Ta})\text{O}_6$ nano-precipitates,” *Sci. Rep.*, vol. 6, Feb. 2016, Art. no. 21188.
- [10] G. Ercolano *et al.*, “State-of-the-art flux pinning in $\text{YBa}_2\text{Cu}_3\text{O}_{7-\delta}$ by the creation of highly linear, segmented nanorods of $\text{Ba}_2(\text{Y/Gd})(\text{Nb/Ta})\text{O}_6$ together with nanoparticles of $(\text{Y/Gd})_2\text{O}_3$ and $(\text{Y/Gd})\text{Ba}_2\text{Cu}_4\text{O}_8$,” *Supercond. Sci. Technol.*, vol. 24, no. 9, Aug. 2011, Art. no. 095012.
- [11] P. Cayado *et al.*, “Epitaxial $\text{YBa}_2\text{Cu}_3\text{O}_{7-x}$ nanocomposite thin films from colloidal solutions,” *Supercond. Sci. Technol.*, vol. 28, no. 12, Nov. 2015, Art. no. 124007.
- [12] L. Civale, “Vortex pinning and creep in high-temperature superconductors with columnar defects,” *Supercond. Sci. Technol.*, vol. 10, no. 7A, pp. A11–A28, Apr. 1997.
- [13] M. Sparing *et al.*, “Artificial pinning centres in YBCO thin films induced by substrate decoration with gas-phase-prepared Y_2O_3 nanoparticles,” *Supercond. Sci. Technol.*, vol. 20, no. 9, pp. S239–S246, Aug. 2007.
- [14] J. Eickemeyer *et al.*, “Nickel-refractory metal substrate tapes with high cube texture stability,” *Supercond. Sci. Technol.*, vol. 14, no. 3, pp. 152–157, Mar. 2001.
- [15] J. B. Nelson and D. P. Riley, “An experimental investigation of extrapolation methods in the derivation of accurate unit-cell dimensions of crystals,” *Proc. Phys. Soc.*, vol. 57, no. 3, pp. 160–177, May 1945.
- [16] International Centre for Diffraction Data, Newtown Park, PA, USA, PDF cards 00-038-1433 ($\text{YBa}_2\text{Cu}_3\text{O}_7$), 00-053-0101 (Ba_2YTaO_6), 00-024-1042 (Ba_2YNbO_6).
- [17] F. Hengstberger, M. Eisterer, M. Zehetmayer, and H. W. Weber, “Assessing the spatial and field dependence of the critical current density in YBCO bulk superconductors by scanning Hall probes,” *Supercond. Sci. Technol.*, vol. 22, no. 2, Jan. 2009, Art. no. 025011.
- [18] R. Nast *et al.*, “Influence of laser striations on the properties of coated conductors,” *J. Phys. Conf. Ser.*, vol. 507, no. 2, 2014, Art. no. 022023.
- [19] M. Sieger *et al.*, “ BaHfO_3 -doped thick $\text{YBa}_2\text{Cu}_3\text{O}_{7-\delta}$ films on highly alloyed textured Ni-W tapes,” *IEEE Trans. Appl. Supercond.*, vol. 25, no. 3, Jun. 2015, Art. no. 6602604.
- [20] R. Hühne *et al.*, “Application of textured highly alloyed Ni-W tapes for preparing coated conductor architectures,” *Supercond. Sci. Technol.*, vol. 23, no. 3, Feb. 2010, Art. no. 034015.
- [21] A. Tsurata *et al.*, “Effect of BaHfO_3 introduction on the transport current at the grain boundaries in $\text{SmBa}_2\text{Cu}_3\text{O}_y$ films,” *Appl. Phys. Exp.*, vol. 8, no. 3, Feb. 2015, Art. no. 033101.
- [22] J. Eickemeyer *et al.*, “Elongated grains in textured substrate tapes and their effect on transport currents in superconductor layers,” *Appl. Phys. Lett.*, vol. 90, no. 1, Jan. 2007, Art. no. 012510.

Repository KITopen

Dies ist ein Postprint/begutachtetes Manuskript.

Empfohlene Zitierung:

Sieger, M.; Pahlke, P.; Hänsch, J.; Sparing, M.; Bianchetti, M.; MacManus-Driscoll, J.; Lao, M.; Eisterer, M.; Meledin, A.; Van Tendeloo, G.; Nast, R.; Schultz, L.; Holzapfel, B.; Hühne, R.

[Ba₂Y\(Nb/Ta\)O₆-Doped YBCO Films on Biaxially Textured Ni-5at.% W Substrates.](#)

2016. IEEE transactions on applied superconductivity, 26

[doi: 10.554/IR/1000055502](#)

Zitierung der Originalveröffentlichung:

Sieger, M.; Pahlke, P.; Hänsch, J.; Sparing, M.; Bianchetti, M.; MacManus-Driscoll, J.; Lao, M.; Eisterer, M.; Meledin, A.; Van Tendeloo, G.; Nast, R.; Schultz, L.; Holzapfel, B.; Hühne, R.

[Ba₂Y\(Nb/Ta\)O₆-Doped YBCO Films on Biaxially Textured Ni-5at.% W Substrates.](#)

2016. IEEE transactions on applied superconductivity, 26 (3), 7500305.

[doi:10.1109/TASC.2016.2539254](#)

Lizenzinformationen: [KITopen-Lizenz](#)